Science
AAAS

Realizing All-Spin–Based Logic Operations Atom by Atom
Alexander Ako Khajetoorians, *et al.*
Science **332**, 1062 (2011);
DOI: 10.1126/science.1201725

Science (print ISSN 0036-8075; online ISSN 1095-9203) is published weekly, except the last week in December, by the American Association for the Advancement of Science, 1200 New York Avenue NW, Washington, DC 20005.

Realizing All-Spin–Based Logic Operations Atom by Atom

Alexander Ako Khajetoorians, Jens Wiebe,* Bruno Chilian, Roland Wiesendanger

An ultimate goal of spintronic research is the realization of concepts for atomic-scale all-spin–based devices. We combined bottom-up atomic fabrication with spin-resolved scanning tunneling microscopy to construct and read out atomic-scale model systems performing logic operations. Our concept uses substrate-mediated indirect exchange coupling to achieve logical interconnection between individual atomic spins. Combined with spin frustration, this concept enables various logical operations between inputs, such as NOT and OR.

In conventional silicon-based information technology, bits of information are represented by charge stored in capacitors and processed by transistor-based switches. The looming fundamental scaling limits of this technology toward nanometer-sized devices (*1*) has led to an exploration of a variety of alternative computation schemes ranging from molecular quantum dot cellular automata (*2*, *3*) and molecular cascades (*4*), to spin capacitors (*5*), magnetic quantum dot cellular automata (*6*), magnetic domain wall devices (*7*–*9*), and eventually strategies for quantum computation (*10*, *11*). In the pursuit of highly energy-efficient and high-speed devices that are compatible with nonvolatile storage technology, spintronic concepts offer much promise (*12*). Such concepts harness the spin degree of freedom of nuclei, electrons, atoms, molecules, or magnetic films rather than the charge of electrons to store and process information. Although many of the proposed devices require spin to charge conversion in order to operate (*5*), it is desirable to have an all-spin–based concept that does not involve any flow of charge. The realization of corresponding model systems with dimensions on the atomic scale is so far lacking.

The tip of a scanning tunneling microscope (STM) has emerged as the tool that can be used to fabricate atomic-scale structures in a bottom-up fashion (*13*–*15*). Moreover, two complementary STM-based methods, spin-polarized scanning tunneling spectroscopy (SP-STS) (*16*) and inelastic STS (*17*), have become the analogs of magnetometry and spin resonance pushed to the single-atom limit. SP-STS has demonstrated the possibility of using the distance-dependent Ruderman-Kittel-Kasuya-Yosida (RKKY) coupling mediated by conduction electrons in metallic substrates to tailor the sign and strength of the magnetic coupling between atomic spins (*18*) as well as with patches of ferromagnetic islands (*16*).

We applied these techniques to realize a model system for logical operations that uses atomic spins of adatoms adsorbed on a nonmagnetic metallic surface and their mutual RKKY interaction in order to transmit and process information (Fig. 1). The atoms have two different states, **0** or **1**, depending on the orientation of their magnetization (down or up, respectively). They are constructed to form antiferromagnetically RKKY-coupled chains ("spin leads") that transmit the information of the state of small ferromagnetic islands ("input islands") to the gate region. The gate region, which comprises two "end atoms" from each spin lead and an "output atom," forms the core where the logic operation is performed. The states of the inputs and the resultant state of the output atom are read out by a scannable magnetic nano-electrode—the magnetic tip of a STM—in a tunneling magnetoresistance device geometry (*16*). Although the STM is used to construct and characterize the device, the tunneling current is not essential for performing the given logic operation. The states of the inputs can be switched independently by external magnetic field pulses $\vec{B}_{pulse}$. Based on an all-spin concept, this model device is principally nonvolatile and functions without the flow of electrons, promising an inherently large energy efficiency.

Triangular cobalt islands grown on the atomically clean (111) surface of a copper single crystal have a remnant mono-domain magnetization oriented perpendicular to the surface ("out-of plane") and serve as nonvolatile input bits (*19*, *20*). For atomic spins, we chose Fe atoms adsorbed at low temperature onto the same surface (fig. S1) (*19*). As a result of a strong magnetic anisotropy energy of ≈1 meV (*21*) and a negligible thermal energy of $k_BT = 25$ μeV (where k_B is the Boltzmann constant) determined by the measurement temperature (T = 0.3 K) (*22*), each atomic spin is constricted to the two states oriented maximally out-of-plane. Isolated Fe atoms are therefore flipping randomly between these two states. However, if an Fe atom sits close to a Co island or another stabilized atom, the distance-dependent oscillatory RKKY interaction stabilizes its spin into one of these two states. This RKKY interaction is on the order of 0.1 meV, and its distance dependence was determined as described in (*16*, *18*) for pairs of Fe atoms and Fe atoms close to Co islands (*19*). As the first step, the atomic spin of the first atom in a spin lead has to be magnetically coupled to the input island by means of the RKKY interaction, which was achieved by using the magnetic tip (*19*) of the STM to move the atom (*13*, *23*) toward the input island to an adequate coupling distance. Figure 2A shows magnetic imaging of several Fe atoms positioned in the vicinity of an input island (α) recorded with a chromium-coated (*19*) STM tip that is sensitive to the out-of-plane component of the magnetization of both the islands and the atoms (yellow or blue indicates the magnetic state **1** or **0**, parallel or antiparallel to the tip magnetization $\vec{M}$, respectively). The first atom was positioned at the

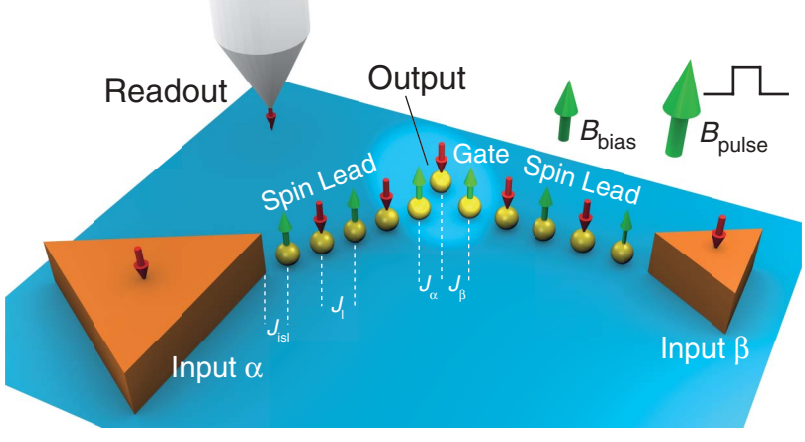

Fig. 1. Device concept for an atomic-spin–based logic gate. Two chains ("spin leads"), which are antiferromagnetically coupled magnetic atoms (yellow spheres) on a nonmagnetic metallic substrate with interatomic couplings J_l, are exchange-coupled by J_{isl} to two "input islands" (α, β) of different size, consisting of patches of ferromagnetic layers. The "end atom" of each spin lead and the final "output atom" form a magnetically frustrated triplet with an antiferromagnetic coupling of $J_\alpha = J_\beta$ which constitutes the logic gate. The spin lead parity (even/odd number of atoms) and the constant biasing field $\vec{B}_{bias}$ determine the logical operation of the gate, and the field pulse $\vec{B}_{pulse}$ is used to switch the inputs. The magnetic tip of a STM is used to construct and characterize the device.

Institute of Applied Physics, Hamburg University, Jungiusstrasse 11, D-20355 Hamburg, Germany.

*To whom correspondence should be addressed. E-mail: jwiebe@physnet.uni-hamburg.de

top corner of the island at a distance where the coupling is antiferromagnetic with an exchange energy of $|J_{isl}| \approx 0.3 - 0.35$ meV. This coupling varies slightly depending on the exact distance to the input island and on the local geometry of the island corner [supporting online material (SOM) text and fig. S2]. Thus, while the input island is in state **1** the atom is in state **0**. In the next step, the spin lead is built atom-by-atom by subsequently adding Fe atoms with an interatomic distance d = 0.923 nm, where the interatomic exchange coupling is antiferromagnetic ($|J_{isl}| \approx 0.1$ meV) (Fig. 2, A to E) for spin leads with lengths of up to six atoms. The read-out signal from the end atom in each spin lead (Fig. 2F) shows that the output is digital and affirms or negates the state of the input for spin leads with an even or odd number of atoms, respectively; thus, odd-number spin leads transmit the inverted input, performing a NOT function.

The next step is to select a second input island (β) in proximity to the first and transmit its state to a position close to the end atom of the first lead by constructing a second spin lead. Both constructed spin leads are illustrated in Fig. 3A, one with six atoms and the other with four atoms, each coupled to the corner of a separate input. The inputs have been chosen to have drastically different sizes and consequently different coercivities $B^{\alpha}_{coe} \approx 1.75$ T and $B^{\beta}_{coe} \approx 0.4$ T, so that their state can be switched independently by using magnetic field pulses $\vec{B}_{pulse}$ of different strength and polarity. Figure 3B shows the device after the application of $B_{pulse} \approx -0.4$ T, which switches input β from state **1** to **0** while input α stays in state **0**. Upon reversal of the input, each atom in the six-atom spin lead reverses its state, and the end atom again affirms the state of the input. There is no obvious change to the opposite lying spin lead coupled to the other input, indicating minimal cross talk between the spin leads.

The last step necessary to construct a logical gate by using our proposed concept is to place an output atom at an appropriate distance between the end atoms of both spin leads, that is, construct the gate region. The interplay between the exchange couplings J_α and J_β of the output atom and J_l of both spin leads (Fig. 1) is pivotal in determining whether the device works as a logical gate. Given that the exchange interaction between each spin lead and its island J_{isl} dominates, and that the mutual interaction between the end atoms in both leads is smaller than J_1, which is a prerequisite for device functionality, there are three principal cases to consider: (i) the "extended chain" case, where $J_l \geq J_\alpha > J_\beta$ or $J_\alpha > J_l > J_\beta$; (ii) the "cross-talk" case, where $J_\alpha \geq J_\beta \geq J_l$; and (iii) the "frustration" case, where $J_l > J_\alpha = J_\beta$. For case (i), the output is only sensitive to the state of one input, and thus the device works as an affirmation or negation of its corresponding input, similar to the demonstration in Fig. 2. For case (ii), the two spin leads cannot be regarded as independent and influence each other. In order to realize basic logical functions, this is undesirable because each end atom of each spin lead should solely reflect its corresponding input. Only the frustration case (iii) offers a viable and flexible solution in the following way: If the two end atoms of each spin lead are in the same state, the output atom will negate that state. If the two end atoms are in opposite states, the output atom is magnetically frustrated, yielding a degeneracy because it wants to align antiparallel to both end atoms. This frustration can easily be broken by applying a biasing magnetic field $\vec{B}_{bias}$, which is weak enough not to change either of the spin lead states or modify the input state but strong enough for the frustrated output to energetically favor one state.

The realization of such a gate using two odd length spin leads is illustrated in Fig. 4, A to D. The interatomic spacing of both spin leads is d = 0.923 nm, resulting in antiferromagnetic coupling $|J_l| \approx 0.1$ meV, and the gate is an equilateral triplet with an interatomic distance of d = 1.35 nm, resulting in antiferromagnetic coupling $|J_\alpha| = |J_\beta| \approx 0.025$ meV. The two inputs are switched independently from Fig. 4A to Fig. 4D by applying $\vec{B}_{pulse}$ of appropriate strength and direction. Each spin lead adjusts to its corresponding input independently of the other input state. The output is in the **0** (**1**) state when both inputs are in the **0** (**1**) state corresponding to the negation of the input by the end atoms of the odd spin leads. If the inputs are in different states, the output aligns parallel to B_{bias} = +50 mT (state **1**), and the device thus works as an OR gate (see truth values below Fig. 4, A to D).

The major loop magnetization curves (*18*, *21*) of both input islands (α, β) as well as of the output atom are shown in Fig. 4, E and F. Clearly, input α has a much larger coercive field ($B^{\alpha}_{coe} \approx 1.75$ T) than that of input β ($B^{\beta}_{coe} \approx 0.4$ T), which allows for a large range of magnetic field pulses ($0.4\ T \leq |B_{pulse}| \leq 1.75\ T$) that can switch the inputs independently. During the initial downward sweep (blue markers), both inputs and the output are in state **1** until the field overcomes the exchange interaction between the output atom and the two end atoms at $B_{crit} = -m \times |J_\alpha + J_\beta| \approx -3.5\mu_B \times 0.05$ meV = –0.25 T (*18*) [where m is the magnetic moment of the Fe atom (*21*)], where the output is forced into state **0**. In the upwards sweep (red markers), the output does not revert back to state **1** until the field once again overcomes $B_{crit} \approx +0.25$ T. Thus, during this major loop the inputs are only inverted

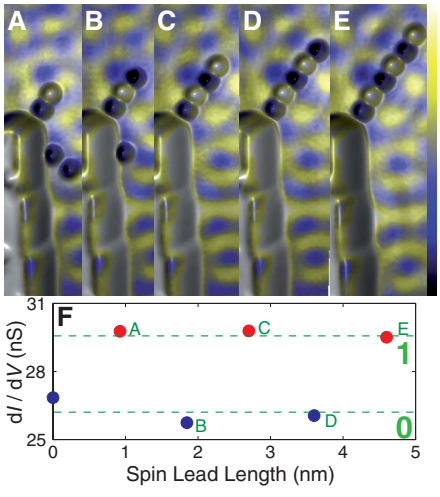

Fig. 2. Construction and read-out of a spin lead. (**A** to **E**) Top view three-dimensional (3D) topographs colored with simultaneously measured spin-resolved d*I*/d*V* map of spin leads of different lengths [two (A) to six (E) atoms] constructed from antiferromagnetically coupled Fe atoms with interatomic distance d = 0.923 nm on Cu(111). The first atom in the spin lead is magnetically stabilized by the corner of a triangular Co input island (bottom left). The color on top of each atom or island reflects its magnetization state (**0**, blue; **1**, yellow; color bar ranges from 26.5 to 30.4 nS). (**F**) d*I*/d*V* signal averaged on the end atom of each lead in (A) to (E) as a function of spin lead length illustrating the digital output of the end atom. B_{bias} = +200 mT; V_{sample} = −10 mV; I_t = 600 pA; V_{mod} = 5 mV [root mean square (rms)].

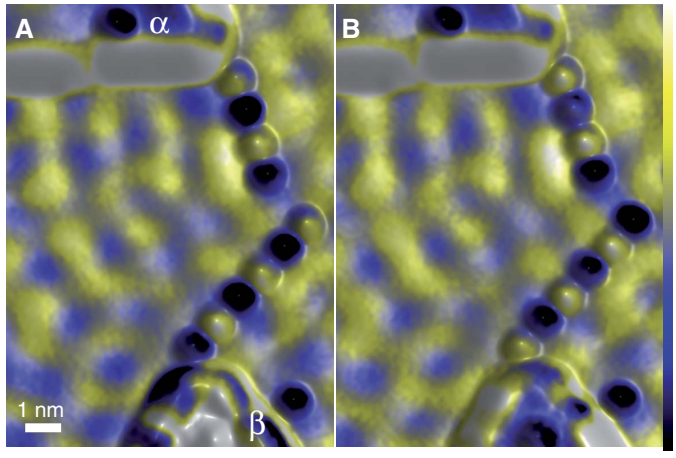

Fig. 3. (**A** to **B**) Switching of a spin lead. Each of the two antiferromagnetic spin leads (d = 0.923 nm) is magnetically coupled to the corner of one of the two Co input islands having different sizes (α, β). By applying $|B_{pulse}| \approx 0.4$ T, the magnetization of the smaller input island (β) is reversed from (A) **1** to (B) **0**. The six-atom spin lead accordingly transmits the information to its end atom, whereas the four-atom spin lead coupled to the input island α remains unaffected. B_{bias} = +200 mT; V_{sample} = −10 mV; I_t = 600 pA; V_{mod} = 5 mV (rms); color bar ranges from 24 to 29 nS.

relative to each other at a field above $|B_{crit}|$, and consequently the frustrated situation in which the output is aligned with $\vec{B}_{bias}$ does not occur. As shown by magnetization curves of the other atoms in the two spin leads (SOM text and fig. S2), the detailed couplings within each spin lead are more complex because of a residual exchange interaction of atoms within each spin lead with the corresponding input island and because of residual cross talk between the leads. Therefore, the magnetic signal strength of each atom in the lead and of the output atom is different. However, we can conclude that as long as $0 < B_{bias} < B_{crit}$ the device works as an OR gate.

Our proposed scheme is quite flexible. In the above example of the OR gate, the orientation of $\vec{B}_{bias}$ and $\vec{M}_{tip}$ was chosen to be parallel. The logical function is changed if this relative orientation is reversed. The logical function can be changed as well by using different combinations of even- and odd-length spin leads. All possible combinations and the resulting logical functions are summarized in Table 1.

There are several open issues to be solved before these realized model systems can be scaled to a larger logic device architecture. In order to drive additional gates, it remains to be demonstrated how to realize an output spin lead and a fan-out by coupling two spin leads to the end atom of an output spin lead. This might be challenging because the magnetic stability of the spin leads will decrease as a function of their length, which would increase the error rate of the end atoms. However, the distance dependence of the RKKY interaction inherently offers flexibility, giving this concept extensive versatility. Although rather weak antiferromagnetic couplings were used for the realized model gate, combinations of antiferromagnetic and stronger ferromagnetic couplings can be achieved by a proper tuning of the interatomic distances in order to stabilize the spin leads. For example, by linking the Fe atoms with Cu adatoms the interaction strength can be increased by an order of magnitude (*24*). For the logical operations presented here, we made use of quasiclassical magnetic moments pointing either up or down. Implementation of quantum mechanical spins with more than two states (*25*) may present an intriguing extension of our demonstrated concept by providing a larger number of states for each atom and could potentially lead to the realization of model systems for quantum information processing.

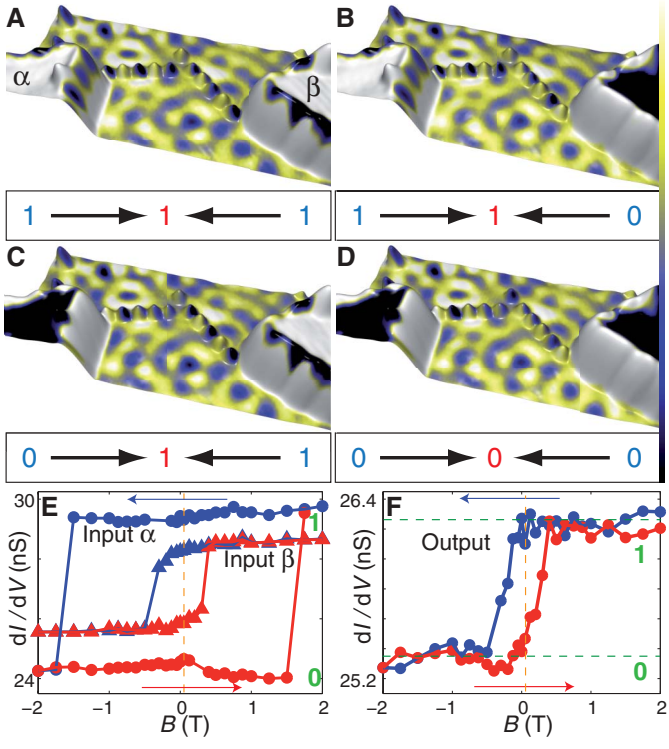

Fig. 4. OR gate. (**A** to **D**) Side view 3D topographs colored with simultaneously measured spin-resolved d*I*/d*V* map of the device for all four possible input permutations (color bar ranges from 24.7 to 26.9 nS). The spin leads have an interatomic distance of $d = 0.923$ nm, and the antiferromagnetic gate triplet is equilateral with $d = 1.35$ nm. By applying out-of-plane magnetic field pulses of different strength and direction [(A) → (B): $B_{pulse} = -0.39$ T, (B) → (C): $B_{pulse} = -2$ T, +0.75 T, (C)→(D): $B_{pulse} = -0.385$ T], each input (α, β) can be controllably switched, and the two spin leads transmit the information to their end atoms. The output atom in the gate triplet reflects the logical operation of the inputs (in the truth table, states of the inputs are labeled blue and of the output red). The biasing field B_{bias} = +50 mT favors the **1** state of the output atom. (**E** and **F**) Major loop magnetization curves of (E) input α (dots), input β (triangles), and (F) output atom of the OR gate (blue symbols indicate downward sweep and red symbols indicate upward sweep). The saturation magnetization values in the two states are labeled **0** and **1** and marked with dashed horizontal lines in (F). The dashed vertical line corresponds to B_{bias}. $V_{sample} = -10$ mV; $I_t = 600$ pA; $V_{mod} = 5$ mV (rms).

Table 1. Possible logical expectations as a function of the relative orientation of biasing field on magnetization, and of the parity of each spin lead.

	α, β odd	α, β even	α even, β odd	α odd, β even
$\vec{B}_{bias} \uparrow\uparrow \vec{M}_{tip}$	OR	NAND	α → β	α ← β
$\vec{B}_{bias} \uparrow\downarrow \vec{M}_{tip}$	AND	NOR	α ↚ β	α ↛ β

References and Notes

1. D. Hisamoto *et al.*, *IEEE Trans. Electron. Dev.* **47**, 2320 (2000).
2. C. S. Lent, P. D. Tougaw, *Proc. IEEE* **85**, 541 (1997).
3. I. Amlani I *et al.*, *Science* **284**, 289 (1999).
4. A. J. Heinrich, C. P. Lutz, J. A. Gupta, D. M. Eigler, *Science* **298**, 1381 (2002).
5. B. Behin-Aein, D. Datta, S. Salahuddin, S. Datta, *Nat. Nano.* **5**, 266 (2010).
6. A. Imre *et al.*, *Science* **311**, 205 (2006).
7. D. A. Allwood *et al.*, *Science* **309**, 1688 (2005).
8. P. Xu *et al.*, *Nat. Nano.* **3**, 97 (2008).
9. S. S. P. Parkin, M. Hayashi, L. Thomas, *Science* **320**, 190 (2008).
10. D. Loss, D. P. DiVincenzo, *Phys. Rev. A* **57**, 120 (1998).
11. P. Neumann *et al.*, *Nat. Phys.* **6**, 249 (2010).
12. S. A. Wolf *et al.*, *Science* **294**, 1488 (2001).
13. D. M. Eigler, E. K. Schweizer, *Nature* **344**, 524 (1990).
14. F. J. Ruess *et al.*, *Small* **3**, 563 (2007).
15. C. R. Moon, L. S. Mattos, B. K. Foster, G. Zeltzer, H. C. Manoharan, *Nat. Nano.* **4**, 167 (2009).
16. F. Meier, L. Zhou, J. Wiebe, R. Wiesendanger, *Science* **320**, 82 (2008).
17. A. J. Heinrich, J. A. Gupta, C. P. Lutz, D. M. Eigler, *Science* **306**, 466 (2004).
18. L. Zhou *et al.*, *Nat. Phys.* **6**, 187 (2010).
19. Materials and methods are available as supporting material on *Science* Online.
20. O. Pietzsch, A. Kubetzka, M. Bode, R. Wiesendanger, *Phys. Rev. Lett.* **92**, 057202 (2004).
21. A. A. Khajetoorians *et al.*, *Phys. Rev. Lett.* **106**, 037205 (2011).
22. J. Wiebe *et al.*, *Rev. Sci. Instrum.* **75**, 4871 (2004).
23. M. F. Crommie, C. P. Lutz, D. M. Eigler, *Science* **262**, 218 (1993).
24. O. O. Brovko, P. A. Ignatiev, V. S. Stepanyuk, P. Bruno, *Phys. Rev. Lett.* **101**, 036809 (2008).
25. C. F. Hirjibehedin, C. P. Lutz, A. J. Heinrich, *Science* **312**, 1021 (2006).

Acknowledgments: Financial support from the European Research Council Advanced Grant "FURORE" by the Deutsche Forschungsgemeinschaft via the SFB668, the Graduiertenkolleg 1286 "Functional Metal-Semiconductor Hybrid Systems," as well as from the Cluster of Excellence "Nanospintronics" funded by the Forschungs- und Wissenschaftsstiftung Hamburg is gratefully acknowledged. The authors thank S. Lounis, M. Potthoff, and R. Wieser for extensive discussions.

Supporting Online Material

www.sciencemag.org/cgi/content/full/science.1201725/DC1
Materials and Methods
SOM Text
Figs. S1 and S2
References

12 December 2010; accepted 6 April 2011
Published online 5 May 2011;
10.1126/science.1201725